Nanoscale Mechanisms of Evaporation, Condensation and Nucleation in Confined Geometries

Nobuo Maeda* and Jacob N. Israelachvili

Department of Chemical Engineering and Materials Department, University of California, Santa Barbara, California 93106

Received: August 30, 2001; In Final Form: February 6, 2002

Capillary condensation, evaporation, and nucleation have been extensively studied for decades, but many fundamental questions remain unresolved. Compared to capillary condensation (e.g., pore filling), the reverse phenomenon of capillary evaporation (e.g., pore emptying) has received little attention, mainly due to a lack of suitable experimental techniques. We present the first detailed ångstrom-level measurement of evaporation of a cyclohexane condensate (liquid bridge) in a slitlike nanopore bounded by two mica surfaces of adjustable gap separation. As the separation is increased beyond the equilibrium (Kelvin) diameter, the liquid condensate evaporates, but we also find that the density becomes nonuniform across the condensate—falling significantly over a few microns from the edge of the meniscus. As the evaporation proceeds in time, the nonuniform density falls gradually and continuously from liquid to vapor, ultimately attaining that of the vapor. If the gap distance is decreased before the condensate has fully disappeared, then recondensation takes place via a gradual and continuous increase in the density without hysteresis, i.e., reversibly. Our findings suggest a new mechanism for capillary evaporation and nucleation and, possibly, for the hydrophobic interaction.

When two surfaces are brought into contact in the undersaturated vapor of a liquid that wets or partially wets the surfaces ($\theta = 0°$ or $0 < \theta < 90°$, respectively, where θ is the contact angle), molecules from the vapor capillary condense around the contact points, growing into large liquid condensates until, at equilibrium, their surfaces have a concave Kelvin radius, r_K, given by the Kelvin equation[1] in terms of the vapor pressure P and liquid surface tension. The existence of a liquid condensate or bridge between two surfaces also produces an attractive capillary force between them.[1] Capillary condensation and capillary forces play a central role at the nanoscopic through to the macroscopic levels in everyday processes such as nucleation, adsorption on porous materials, particle adhesion and friction in vapors (e.g., humid air), and in oil recovery.[2] Because the crucial steps of nucleation or condensation are essentially nonequilibrium processes, occurring rapidly and at the molecular level, it has been difficult to study capillary effects in detail, and many outstanding experimental and theoretical questions remain unresolved since they were first noted long ago by the pioneers of this subject, such as Maxwell.[3] Whereas most experimental studies have focused on the *formation* of condensates such as the nucleation and condensation of droplets or liquid bridges, here we have also studied the reverse process, viz., the evaporation or *disappearance* of a bulk liquid phase.

To model a slitlike pore of adjustable width H a Surface Forces Apparatus (SFA)[4] was used in which two rigidly held molecularly smooth curved surfaces of mica coexisted with a bulk reservoir of cyclohexane vapor of known relative vapor pressure, P/P_0 (Figure 1A). Cyclohexane is a very common, well-characterized liquid that has been used in fundamental studies of liquids, including earlier SFA work on capillary condensation by Fisher and Israelachvili that verified the Kelvin and Laplace equations for highly curved surfaces *at equilibrium*,[5−8] and some of the earliest measurements of oscillatory solvation forces between surfaces.[9] The separation H could be controlled and measured to 1 Å. In addition, the refractive index n as a function of the bridge (condensate) radius x could be measured interferometrically with Fringes of Equal Chromatic Order (FECO)[10] using the standard three-layer interferometer equation.[11] The reference wavelengths used for computing H

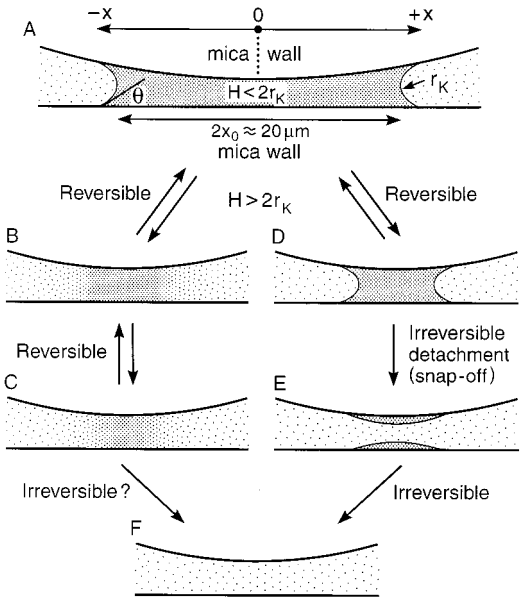

Figure 1. (**A**) The crossed-cylinder geometry of the mica surfaces in the surface forces apparatus is equivalent to a macroscopic sphere (of radius ∼2 cm) approaching a flat surface, which is a good model for a slitlike pore. The distance H was adjustable in the range 0−1000 nm (above and below the Kelvin diameters $2r_K$), and the diameters of the condensates $2x$ varied in the range 100−0 μm. For cyclohexane liquid on mica the contact angle is $\theta < 6°$ ($\cos\theta \approx 0.995$).[7] (**B**, **C**, **F**) Stages in the evaporation of cyclohexane liquid condensates as visualized and measured with Fringes of Equal Chromatic Order (FECO), shown in Figure 2. (**D**, **E**, **F**) "Classic" picture of the stages in the evaporation of a liquid condensate.[16]

* To whom correspondence should be addressed. E-mail: nobuo@engineering.ucsb.edu. Fax: 805-893-7870. Tel: 805-893-5268.

10.1021/jp013365u CCC: $22.00
Published on Web 03/19/2002

and the refractive index profiles are those corresponding to flat surface-surface contact at $H = 0$. Different P/P_0 conditions were studied by equilibrating the SFA chamber with different binary liquid mixtures of up to ~4 mol % squalane (Sigma-Aldrich, 99% pure) as the involatile solute in cyclohexane (Fisher Scientific, 99.9% pure). A control experiment with pure (100 mol %) squalane showed no measurable squalane adsorption on the mica surfaces during the time scales of the experiments.

One of us has previously shown that the Kelvin equation holds down to the scale of this study.[6] Five precise values of P/P_0 were obtained by first measuring the equilibrium Kelvin diameters $2r_K$ of the capillary condensed annuli of cyclohexane around the contacting mica surfaces ($\theta < 6°$[7]) from the discontinuities in the interference fringes (Figure 2A), then using the Kelvin equation,[6] to give $P/P_0 = 0.992$ ($r_K = 127.5$ nm), 0.938 ($r_K = 17.1$ nm), 0.915 ($r_K = 12.3$ nm), 0.881 ($r_K = 8.7$ nm) and 0.846 ($r_K = 6.5$ nm). At the three lowest vapor pressures and corresponding Kelvin radii, the surfaces jumped apart to $H > 2r_K$ when separated from adhesive contact, and the liquid bridges were too small and evaporated too rapidly for accurate quantitative measurements to be made. The measured refractive indices of these unstable (evaporating) condensates were 1.39 (for $r_K = 12.3$ nm) and 1.31 (for $r_K = 8.7$ nm). For the two highest vapor pressures, the surfaces jumped apart to $H < 2r_K$ and the measured refractive indices of the stable condensates (cf., Figures 1A and 2B) were $n = 1.44$ both at $r_K = 127.5$ nm and $r_K = 17.1$ nm. Below, we concentrate mainly on the results obtained at the second highest vapor pressure ($r_K = 17.1$ nm). All the measurements were carried out at 25.0 °C in the presence of P_2O_5 as drying agent.

At any given vapor pressure P/P_0 or Kelvin radius r_K, the refractive index n of a *stable* condensate (one for which $H < 2r_K$) was found to be uniform across the condensate and independent of H. The refractive index of 1.44, so measured at the two highest vapor pressures, is in reasonable agreement with the literature value of 1.426 for bulk liquid cyclohexane at 20 °C.[12] For H larger than the Kelvin diameter $2r_K$, as the neck radius x of the evaporating condensate falls below about 10 microns, its refractive index starts to fall below the bulk value at the liquid−vapor interface and becomes a function of the lateral radius, i.e., $n = n(x)$, where n is highest at the center, $x = 0$, and decreases monotonically toward the boundary as illustrated in Figures 1B and 2C. Then, just before the condensate disappears, the refractive index of the whole condensate, even at the center, falls rapidly but still continuously until it reaches the value corresponding to pure vapor, as illustrated in Figures 1C and 2D−F. However, at some point between C and F in Figure 1 (or between E and F in Figure 2) the transition ceases to be reversible: reducing H does not lead to the continuous regrowth of the condensate. Instead, the condensate continues to disappear and can only be made to spontaneously reappear by bringing the surfaces into contact again. The time scales for evaporation and nucleation of these micron-sized bridges depend on P/P_0 and H, varying from seconds to ms.

The video-recorded FECO fringes shown in Figure 2 are for the system at $P/P_0 = 0.938$, but the observed qualitative behavior, shown in the middle row of Figure 2, was the same at all the vapor pressures studied. The gradient in the refractive index across the condensate and the speed of its disappearance was larger at lower P/P_0 and higher H values. Immediately before the evaporation is complete, the FECO fringes become visibly continuous from the center of the condensate into the vapor phase (Figure 2E), suggesting that at this stage the "liquid−vapor interface" has become diffuse at the microscopic level. Typical refractive index profiles across the evaporating bridges using the standard three-layer interferometer equation[11] are presented in the third row of Figure 2. Importantly, detailed analysis of the fringe profiles across a disappearing condensate with time readily reveal that in the final stage of disappearance or collapse (between C and F in Figure 1, and E and F in Figure 2) the change in the refractive index is continuous in both space (along x) and time, even though it is now irreversible.

The presence of a refractive index gradient implies, via the Lorentz−Lorenz equation,[13] a density gradient within the liquid condensate of cyclohexane along the radial x-direction. For $H < 2r_K$ the density is uniform across the condensate and equal to the bulk value (Figure 2B). For $H > 2r_K$ it begins to fall reversibly from the edge of the meniscus. Only at the final stage does it fall irreversibly throughout the condensate toward the value for cyclohexane vapor. Concerning the precise molecular rearrangements associated with the density variations inside the condensates, we believe these to be continuous. Thus, we cannot rule out the formation of nanoscopic vapor bubbles or cavities inside the neck during the evaporation or condensation processes; such cavities can lead to boiling, which has been suggested to occur in liquids that are subjected to negative pressures.[14,15] We here merely point out that the formation of subnano-bubbles with sharp liquid−vapor interfaces seems unlikely; in addition, their distribution would have to be highly nonlinear yet continuously and rapidly reversible.

The different stages of evaporation suggested by these results are illustrated in Figure 1, parts A, B, C, and F, which are quite different from the expected or conventional thermodynamic mechanism, shown in Figure 1, parts D and E, in which the liquid−vapor interface remains sharp and well-defined at all stages of the evaporation and which involves an irreversible Laplace instability[16] (snap-off) on detachment, in contrast to the much more continuous and reversible transition actually observed. When the surfaces are moved apart slowly (~Å/sec), our observations and recordings showed no evidence of an *abrupt* snap-off or Laplace instability at any stage of the evaporation (e.g., Figure 1, parts D → E), nor the reverse phenomenon of an abrupt condensation (Figure 1, parts E → D). A study by one of us with involatile liquids showed that such *irreversible* instabilities can occur, but at much larger slit widths H that are also different for the detachment and coalescence processes.[17] However, for such low vapor pressure compounds, the evaporation rate is so slow that the liquid bridge may persist at an H slightly larger than $2r_K$ for hours. Although no experimental study of evaporation of such "involatile" condensates has been reported, they should eventually evaporate if one waits for a sufficiently long time.

It is worth considering what the results tell us about the meaning of thermodynamic, metastable and kinetic equilibrium, about continuous and discontinuous processes or transitions, and about reversibility. Theoretical modelings of highly curved liquid surfaces have been consistent with the classical concept of the Gibbs dividing surface[18] and predict sharp liquid−vapor interfaces under *equilibrium* conditions,[19] as illustrated in Figure 2B. In contrast, evaporation and condensation are intrinsically nonequilibrium, nonergodic, processes that can be understood only when considered as a function of both space *and* time. Thus, the reversibility in the evaporation and recondensation processes that we observe when $H > 2r_K$—i.e., when the liquid condensate is no longer in thermodynamic equilibrium with its vapor—depends on how far *and* how fast the surfaces are moved toward or away from each other. When the surfaces are moved

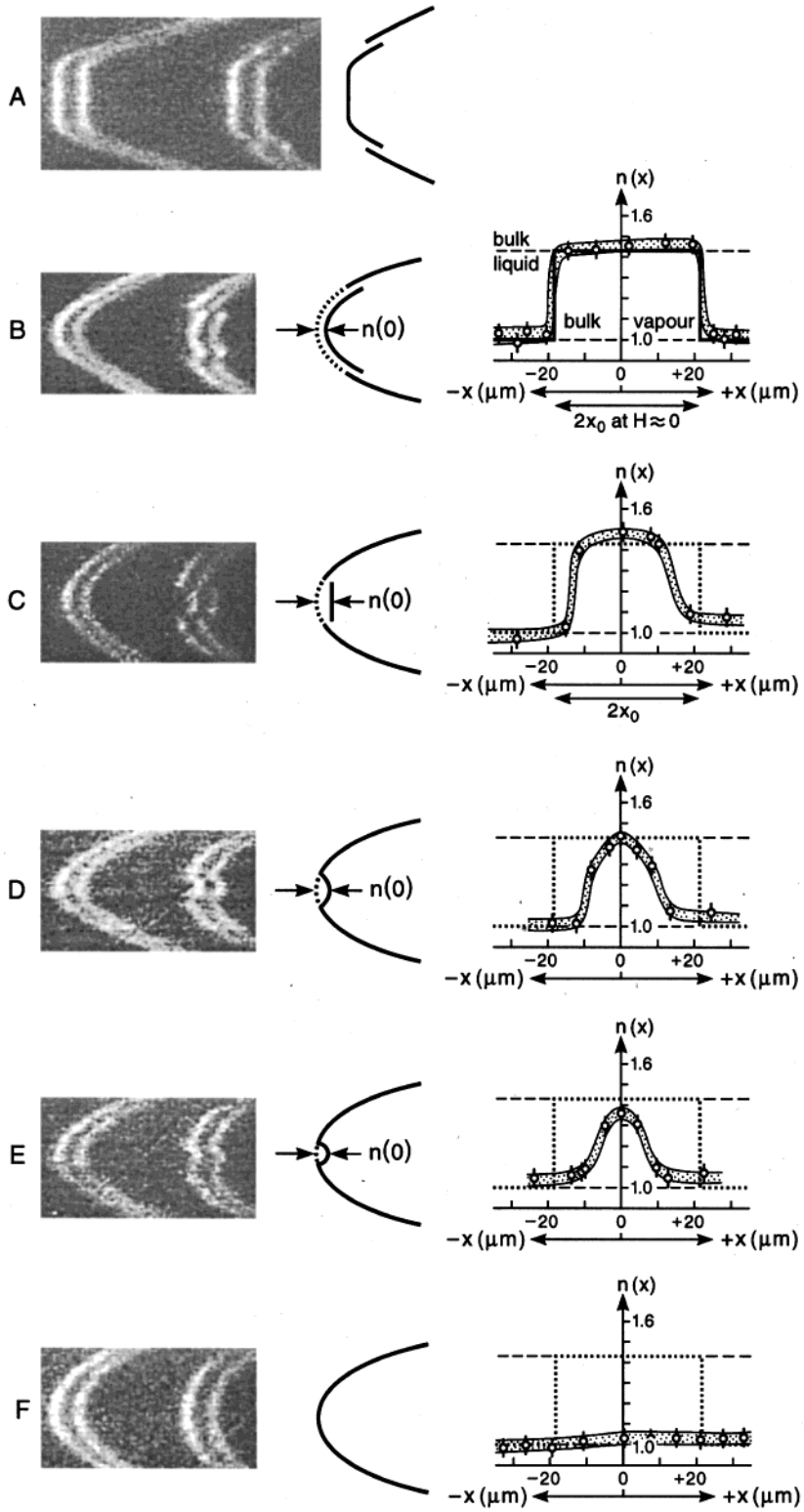

Figure 2. Left row: typical FECO images or spectrograms of adjacent odd-order and even-order fringes (each fringe appears as a doublet due to the birefringence of mica) during evaporation of the cyclohexane condensate. Middle row: schematics of even-order fringes only, which give the refractive index profile $n(x)$ of the condensates,[11] as shown in the right row. The scale in the lateral direction of each spectrogram is in wavelength (longer wavelengths to the right) while in the vertical direction it is in real space units (determined by the magnification of the microscope used to view the surfaces), so the FECO images of the first two rows must be rotated by 90° anticlockwise to match the refractive index profiles in the third row or the schematics of Figure 1.[11] (**A**) FECO images of surfaces in flattened "contact", H ≈ 0, with a thin layer of cyclohexane trapped between them and capillary condensed liquid at the rim. (**B** to **F**) Surfaces separated from contact during progressive evaporation of a liquid condensate. If kept at a fixed H just above $2r_K$, the whole process of evaporation (until the complete disappearance of the condensate) takes a few seconds in the case of $P/P_0 = 0.938$, whereas for larger H and/or lower P/P_0 conditions the evaporation time is much shorter. The error bars shown are the calculated standard deviations of the measurements from a number of video frames. The thickness of the adsorbed films on isolated surfaces (after complete evaporation) was ∼1 nm. Note that reflection and/or refraction at the *sharp* condensate−vapor interface results in a discontinuity (darkening) of the fringes, as in A, B, and C. Note also that cooling effects of the interface due to evaporation would only increase the density at the meniscus compared with the interior of the condensate.

fast enough evaporation or condensation can be reversed continuously in both space and time. By judicious feedback control of the surface separation at the ångstrom-level, we found that it is possible to hold a condensate in a nonequilibrium state, e.g., as in Figures 1C or 2E. It is conceivable that even after the condensate has completely disappeared, recondensation (nucleation) of a bridge could occur 'spontaneously' if the surfaces are held at a finite separation $H < 2r_K$ for a long enough time. Indeed, this would be consistent with the results of earlier measurements of the critical distance or slit width at which capillary condensation occurs spontaneously between two surfaces.[20] The precise values of $n(x)$ varied depending on H, suggesting that there is no well-defined or critical gap distance below which the density begins to change or the interface become diffuse. It is possible that the effect we observe is related to the one described by Heuberger et al.[21] who observed large spatial and temporal fluctuations in confined molecularly thin cyclohexane films at unstable (nonequilibrium) spacings.

Our findings may throw new light on the long-ranged hydrophobic interaction where preexisting or capillary-condensing bubbles and bridges of water vapor or dissolved gas have often been suggested as the cause of the attraction due to the Laplace pressure generated by these bridges.[22,23] Although the previous attempt to measure the reduction of density of water films between two hydrophobic surfaces was unsuccessful,[24] the concept of reduced density has not been discarded (the reduction of water density required to generate the measured hydrophobic force is anyway too small to be detectable using in situ FECO refractive index measurements[24]). The system we have studied is conceptually identical to one in which a vapor cavity "capillary evaporates" out of bulk liquid water to bridge two fully hydrophobic surfaces. This is thermodynamically equivalent to process F → C in Figure 1 with the liquid and vapor phases reversed. Our findings suggest that continuous density gradients that are *monotonic* functions of H may occur spontaneously in a liquid between two surfaces even in the absence of a phase separation. A similar effect may occur in liquid water between two partially hydrophobic surfaces, involving a simple reduction in the density of the liquid below the bulk value prior to a complete liquid−vapor phase separation. The presence of large continuous and monotonic density gradients would generate an attractive potential of mean force (depletion force due to the osmotic pressure change between the surfaces), which have been measured between partially hydrophobic surfaces where $\theta < 90°$ [25,26] and which therefore cannot be accounted for in terms of macroscopic vapor bubbles or cavities.

Acknowledgment. We thank M. M. Kohonen and H. K. Christenson for valuable discussions, G. Carver for technical assistance and D. McLaren for the artwork. This work was supported by a grant from NASA: NAG3-2115.

References and Notes

(1) Hunter, R. J. *Foundations of Colloid Science*; Clarendon Press: Oxford, 1986.

(2) Gelb, L. D.; Gubbins, K. E.; Radhakrishnan, R.; Sliwinska-Bartkowiak, M. *Rep. Prog. Phys.* **1999**, *62*, 1573.

(3) Maxwell, J. C. Capillary Action. In. *Encyclopaedia Britannica*, 9th ed.; 1875; pp 56−71.

(4) Christenson, H. K. *Phys. Rev. Lett.* **1994**, *73*, 1821−1824.

(5) Fisher, L. R.; Israelachvili, J. N. *Nature* **1979**, *277*, 548−549.

(6) Fisher, L. R.; Israelachvili, J. N. *J. Colloid Interface Sci.* **1981**, *80*, 528−541.

(7) Fisher, L. R.; Israelachvili, J. N. *Colloids Surf.* **1981**, *3*, 303−319.

(8) Fisher, L. R.; Israelachvili, J. N. *Chem. Phys. Lett.* **1980**, *76*, 325−328.

(9) Christenson, H. K.; Horn, R. G.; Israelachvili, J. N. *J. Colloid Interface Sci.* **1982**, *88*, 79−88.

(10) Tolansky, S. *Multiple-Beam Interferometry of Surfaces and Films*; Oxford University Press: London, 1949.

(11) Israelachvili, J. N. *J. Colloid Interface Sci.* **1973**, *44*, 259.

(12) *CRC Handbook of Chemistry and Physics*, 80th ed.; CRC press: Boca Raton, 1999−2000.

(13) Born, M.; Wolf, E. *Principles of Optics*, 7th ed.; University Press: Cambridge, 1999.

(14) Derjaguin, B. V. *Zh. Eksp. Teor. Fiz.* **1973**, *65*, 2261−2271.

(15) Derjaguin, B. V.; Prokhorov, A. V. *J. Colloid Interface Sci.* **1981**, *81*, 108−115.

(16) Everett, D. H.; Haynes, J. M. *J. Colloid Interface Sci.* **1972**, *38*, 125−137.

(17) Maeda, N.; Kohonen, M. M.; Christenson, H. K. *J. Phys. Chem.* **2001**, *105*, 5906−5913.

(18) Adamson, A. W.; Gast, A. P. *Physical Chemistry of Surfaces*, 6th ed.; John Wiley & Sons. Inc.: New York, 1997.

(19) Rowlinson, J. S.; Widom, B. *Molecular Theory of Capillarity*; Clarendon Press: Oxford, 1982.

(20) Wanless, E. J.; Christenson, H. K. *J. Chem. Phys.* **1994**, *101*, 4260−4267.

(21) Heuberger, M.; Zach, M.; Spencer, N. D. *Science* **2001**, *292*, 905−908.

(22) Berard, D. R.; Attard, P.; Patey, G. N. *J. Chem. Phys.* **1993**, *98*, 7236−7244.

(23) Yaminsky, V. V.; Ninham, B. W. *Langmuir* **1993**, *9*, 3618−3624.

(24) Kekicheff, P.; Spalla, O. *Langmuir* **1994**, *10*, 1584−1591.

(25) Christenson, H. K.; Claesson, P. M. *Adv. Colloid Interface Sci.* **2001**, *91*, 391−436.

(26) Yoon, R. H.; Flinn, D. H.; Rabinovich, Y. I. *J. Colloid Interface Sci.* **1997**, *185*, 363−370.